Daniel E. Francés,[1] Omar Motiño,[2] Noelia Agrá,[2] Águeda González-Rodríguez,[2,3] Ana Fernández-Álvarez,[1] Carme Cucarella,[4] Rafael Mayoral,[5,6] Luis Castro-Sánchez,[2] Ester García-Casarrubios,[2] Lisardo Boscá,[2,5] Cristina E. Carnovale,[1] Marta Casado,[4,5] Ángela M. Valverde,[2,3] and Paloma Martín-Sanz[2,5]

Hepatic Cyclooxygenase-2 Expression Protects Against Diet-Induced Steatosis, Obesity, and Insulin Resistance

Diabetes 2015;64:1522–1531 | DOI: 10.2337/db14-0979

Accumulation evidence links obesity-induced inflammation as an important contributor to the development of insulin resistance, which plays a key role in the pathophysiology of obesity-related diseases such as type 2 diabetes and nonalcoholic fatty liver disease. Cyclooxygenase (COX)-1 and -2 catalyze the first step in prostanoid biosynthesis. Because adult hepatocytes fail to induce COX-2 expression regardless of the proinflammatory stimuli used, we have evaluated whether this lack of expression under mild proinflammatory conditions might constitute a permissive condition for the onset of insulin resistance. Our results show that constitutive expression of human COX-2 (hCOX-2) in hepatocytes protects against adiposity, inflammation, and, hence, insulin resistance induced by a high-fat diet, as demonstrated by decreased hepatic steatosis, adiposity, plasmatic and hepatic triglycerides and free fatty acids, increased adiponectin-to-leptin ratio, and decreased levels of proinflammatory cytokines, together with an enhancement of insulin sensitivity and glucose tolerance. Furthermore, hCOX-2 transgenic mice exhibited increased whole-body energy expenditure due in part by induction of thermogenesis and fatty acid oxidation. The analysis of hepatic insulin signaling revealed an increase in insulin receptor–mediated Akt phosphorylation in hCOX-2 transgenic mice. In conclusion, our results point to COX-2 as a potential therapeutic target against obesity-associated metabolic dysfunction.

Insulin resistance (IR) plays a key role in the pathophysiology of obesity-related diseases such as type 2 diabetes and nonalcoholic fatty liver disease. IR is the key primary defect underlying the development of type 2 diabetes and is a central component defining the metabolic syndrome. That IR is associated with a state of chronic low-grade inflammation has been demonstrated, and inflammation is assumed to contribute in a major way to its development (1). Besides the fact that IR is characterized by complex interactions between genetic determinants and nutritional factors, it is recognized that mediators synthesized from immune cells and adipocytes are involved in the regulation of insulin action (2). Insulin acts in target cells by binding to its specific receptor and activating a cascade of intracellular signaling events that are altered in inflammation-associated IR (3).

Inflammation induces the expression of a variety of proteins, including prostaglandin–endoperoxide synthase-2, also known as cyclooxygenase (COX)-2, which catalyzes the first step in prostanoid biosynthesis. COX-2 is induced by a variety of stimuli such as growth factors, proinflammatory mediators, hormones, and other cellular

[1]Institute of Experimental Physiology (Instituto de Fisiología Experimental), Consejo Nacional de Investigaciones Científicas y Técnicas, Rosario, Argentina
[2]Institute of Biomedical Research Alberto Sols, Consejo Superior de Investigaciones Científicas-Universidad Autónoma de Madrid, Madrid, Spain
[3]CIBERDEM, Instituto de Salud Carlos III, Madrid, Spain
[4]Biomedical Institute of Valencia, Instituto de Biomedicina de Valencia-Consejo Superior de Investigaciones Científicas, Valencia, Spain
[5]CIBERehd, Instituto de Salud Carlos III, Madrid, Spain
[6]Department of Medicine, University of California, San Diego, La Jolla, CA

Corresponding author: Paloma Martín-Sanz, pmartins@iib.uam.es, or Ángela M. Valverde, avalverde@iib.uam.es.

Received 25 June 2014 and accepted 18 November 2014.

This article contains Supplementary Data online at http://diabetes.diabetesjournals.org/lookup/suppl/doi:10.2337/db14-0979/-/DC1.

D.E.F., O.M., and N.A. contributed equally to this work.

A.M.V. and P.M.-S. share senior authorship.

stresses (4). On one hand, adult hepatocytes fail to induce COX-2 regardless of the proinflammatory stimuli used, and COX-2 is induced only under prolonged aggression as a result of the drop of C/EBP-α (5) or after partial hepatectomy (6). On the other hand, Kupffer, stellate, hepatoma mouse liver cells, and fetal hepatocytes retain the ability to express COX-2 upon stimulation with lipopolysaccharide and proinflammatory cytokines (7).

Previous work has implicated COX-2 in the pathogenesis of obesity and IR. Hsieh et al. (8–10) reported muscle and fat IR improved in rats fed fructose or a high-fat diet (HFD) treated with COX-2 inhibitors. However, Coll et al. (11) found that COX-2 inhibition exacerbated palmitate-induced inflammation and IR in skeletal muscle. Our previous results (12), performed in a model of transgenic (Tg) mice constitutively expressing human COX-2 in hepatocytes (hCOX-2–Tg), demonstrated a protective role of COX-2 against liver apoptosis induced by streptozotocin-mediated hyperglycemia. These findings prompted us to screen the role of COX-2 expression in hepatocytes in a model of IR and altered energy homeostasis induced by HFD. The current study has demonstrated that expression of COX-2 in hepatocytes protects against steatosis, adiposity, inflammation, and hepatic IR in hCOX-2–Tg mice under HFD conditions by improving insulin sensitivity and glucose tolerance, enhancing Akt and AMPK phosphorylation, decreasing protein tyrosine phosphatase-1B (PTP1B) protein levels, and increasing thermogenesis and energy expenditure.

RESEARCH DESIGN AND METHODS

Animal Experimentation

The study used hCOX-2–Tg mice (25–30 g body weight; 3 months) on a B6D2/OlaHsd background along with corresponding age-matched wild-type (Wt) mice (13). Animals were treated according to the Institutional Care Instructions (Bioethical Commission from Spanish Research Council [CSIC], Spain). The hCOX-2–Tg mice and their corresponding Wt littermates were generated by systematic mating of Tg mice with B6D2F1/OlaHsd Wt mice in our animal facilities for more than seven generations.

Insulin Signaling Studies

Wt and hCOX-2–Tg mice fasted for 6 h were intraperitoneally injected with 0.75 units/kg human recombinant insulin and killed 15 min later. The liver was removed, and RNA and total protein extracts were prepared, as previously described (14).

Induction of Liver Steatosis and Obesity by HFD

Wt and hCOX-2–Tg mice were fed a regular chow diet (RCD; A04-10, Panlab, Barcelona, Spain) or a 42% HFD (TD.88137, Harlan Laboratories, Madison, WI) ad libitum for 12 weeks. Some (n = 7) of the hCOX-2–Tg mice fed the HFD were treated intraperitoneally with 10 mg/kg/day DFU, a COX-2 selective inhibitor, five times in a week during all the treatment. During HFD treatment, body weight and food and water intake were recorded every 2 days. After 12 weeks of treatment, animals were killed and the liver, epididymal white adipose tissue (eWAT), inguinal WAT (iWAT), and interscapular brown adipose tissue (BAT) were snap-frozen in liquid nitrogen and stored at −80°C or collected in a solution containing 30% sucrose in PBS or fixed in 10% buffered formalin. Plasma was obtained from the inferior vena cava.

Metabolic Measurements

Metabolic measurements were performed at the beginning of HFD treatment and at the end of week 12. Mice underwent an insulin tolerance test (ITT) and glucose tolerance test (GTT). For the ITT, after mice fasted for 6 h were intraperitoneally injected with 0.75 units/kg human recombinant insulin. Blood glucose was measured from the tail vein at 0, 15, 30, 60, and 90 min. For the GTT, mice fasted for 16 h were intraperitoneally injected with 2 g/kg glucose, and blood samples were taken at 0, 30, 60, and 90 min. Glucose levels were measured with an Accu-Check Glucometer (Roche). The homeostasis model of assessment of IR (HOMA-IR), an index of whole-body IR at the basal state, was calculated as HOMA-IR = (FPI × FPG)/22.5, where FPI is fasting plasma insulin concentration (mU/L) and FPG is fasting plasma glucose (mmol/L).

Indirect Calorimetry

At the end of week 12, independent groups of Wt and hCOX-2–Tg mice (n = 4) were analyzed by indirect calorimetry in a PhenoMaster System (TSE Systems, Bad Homburg, Germany). Mice were acclimated to the test chamber for at least 24 h and were monitored for an additional 48 h. Food and water were provided ad libitum in the appropriate devices and measured by the built-in automated instruments. VO_2 and VCO_2 measurements were taken every 10 min. The respiratory exchange ratio was calculated as: RER = VCO_2/VO_2. Energy expenditure (EE) was calculated as: EE = [3.815 + (1.23 × RER)] × VO_2 × 1.44. Data are the average values obtained in these recordings.

Cold Exposure Experiments

Three-month-old Wt and hCOX-2–Tg mice (n = 8) were acclimated at a temperature of 28°C for 1 week. Then, mice were randomly divided into two groups: one group was exposed to 4°C for 6 h in individual cages and the other group was maintained at 28°C. Mice were killed at the end of the experiment, and BAT, eWAT and iWAT depots were removed and frozen in liquid nitrogen for posterior assays.

Data Analysis

Statistical analyses were performed using SPSS 17 software. Data are expressed as means ± SE. The Student t test was applied whenever necessary, and statistical analysis of the differences between groups was performed by

one-way ANOVA, followed by the Tukey test. $P < 0.05$ was considered statistically significant.

RESULTS

COX-2–Tg Mice Are Protected From HFD-Induced Hepatic Steatosis, Obesity, and IR

To explore whether COX-2 expression in hepatocytes affects glucose tolerance and insulin sensitivity in mice, we used our previously described hCOX-2–Tg mice that constitutively express human COX-2 in hepatocytes under the control of the human apolipoprotein E promoter and its specific hepatic control region, a unique regulatory domain that directs apolipoprotein E expression in the liver (13) and that also lacks macrophage-specific regulatory regions (ME.2 and ME.1) (15), ensuring exclusive expression in liver. Prostaglandin E_2 (PGE_2), the main COX-2–derived prostanoid in the liver, is threefold increased (Supplementary Fig. 1*A* and *B*) (13). The expression of COX-2 in the liver of COX-2–Tg mice was comparable to the levels reached in fetal hepatocytes after stimulation with lipopolysaccharide (5,7) and in liver regeneration after partial hepatectomy (6,16).

Although, no differences in body weight gain were found under the RCD condition (Supplementary Fig. 1*C*), the body weight in hCOX-2–Tg mice fed the HFD did not increase as much as the corresponding Wt littermates, and the eWAT size and liver weight were significantly lower compared with those of the Wt mice (liver weight: 1.29 ± 0.05 g for hCOX-2–Tg and 1.63 ± 0.11 g for Wt; $P < 0.05$) (Fig. 1*A*–*C*). Notably, hCOX-2–Tg mice displayed a 20% lesser body weight gain without significant changes in the initial body weight or in food intake (Fig. 1*D*).

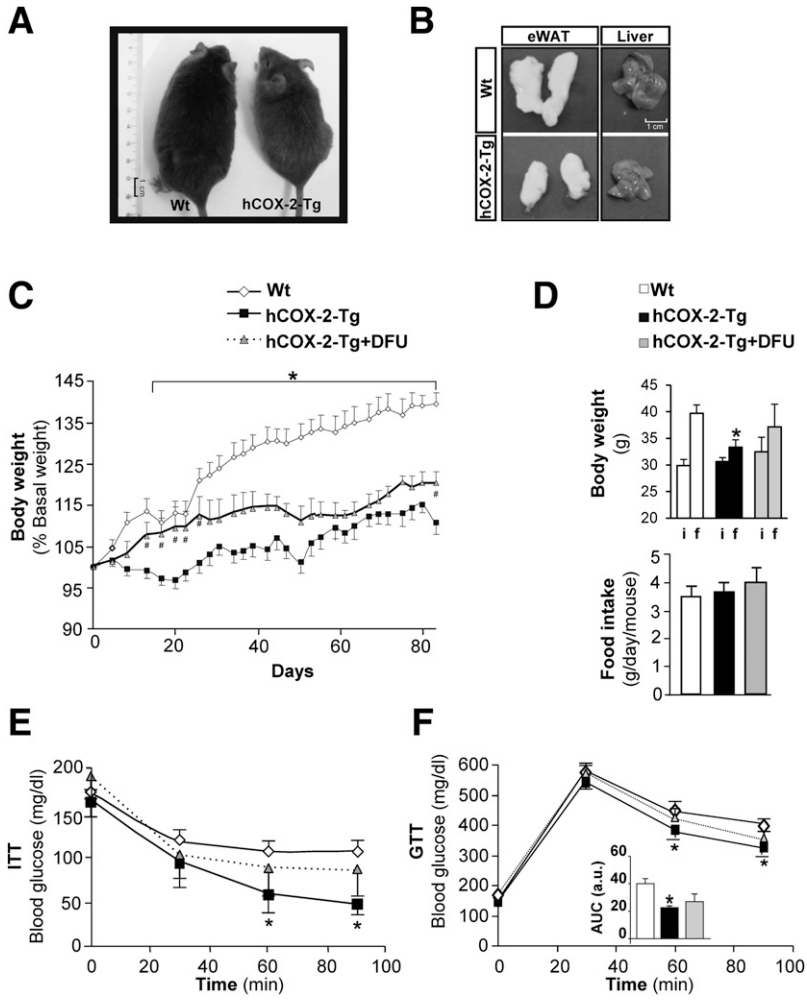

Figure 1—hCOX-2–Tg mice are protected from HFD-induced obesity, insulin, and glucose intolerances. Wt and hCOX-2–Tg mice were fed an HFD ad libitum for 12 weeks. An additional group of hCOX-2–Tg mice was treated with the COX-2 inhibitor DFU five times weekly during all HFD treatment. *A*: Representative photographs of Wt and hCOX-2–Tg mice. *B*: Representative photographs of eWAT and liver from Wt and hCOX-2–Tg mice. *C*: Body weight curve of Wt, hCOX-2–Tg, and hCOX-2–Tg+DFU mice fed an HFD expressed as percentage of basal body weight. Data are expressed as means ± SE ($n = 7$ per group). *$P < 0.05$ vs. Wt; #$P < 0.05$ vs. hCOX-2–Tg. *D*: Initial (i) and final (f) body weight and mean daily food intake. ITT after 6 h fasting (*E*) and GTT after 16 h fasting (*F*) of animals ($n = 6$ per group) after HFD. Graph represents area under the curve (AUC) during GTT. Data are expressed as means ± SE. *$P < 0.05$ vs. Wt.

Interestingly enough, hCOX-2–Tg mice treated with DFU exhibited an intermediate body weight value (Fig. 1*C*). To assess the effect of the HFD on glucose homeostasis, HFD-fed mice underwent GTT and ITT analysis (Fig. 1*E* and *F*). Plasma glucose levels (mg/dL) were similar among genotypes under the HFD condition, at 173.5 ± 6.7 for Wt, 159.2 ± 12.1 for hCOX-2–Tg, and 177.3 ± 21.2 for hCOX-2–Tg+DFU. However, under the HFD condition, hCOX-2–Tg mice displayed enhanced insulin sensitivity (Fig. 1*E*) and glucose tolerance (Fig. 1*F*) compared with the Wt. In addition, treatment of hCOX-2–Tg mice with DFU partially reversed the beneficial effects on glucose homeostasis induced by COX-2–dependent prostaglandins. ITT and GTT also revealed an enhanced insulin sensitivity and glucose tolerance in hCOX-2–Tg versus Wt mice under RCD basal conditions (Supplementary Fig. 1*D* and *E*). The effect of COX-2 expression in hepatic insulin signaling was evaluated in primary hepatocytes. As shown in Supplementary Fig. 2*A*, insulin-induced insulin receptor and Akt phosphorylations were markedly increased in hCOX-2–Tg hepatocytes. Furthermore, when Wt hepatocytes were treated with PGE_2 before insulin stimulation, Akt phosphorylation was increased, and conversely, when hCOX-2–Tg hepatocytes were pretreated with DFU, Akt phosphorylation was decreased, indicating the specificity of COX-2–dependent prostaglandins in the modulation of insulin signaling (Supplementary Fig. 2*B*).

Chronic HFD treatment causes accumulation of lipids in the liver, a process leading to fatty liver disease. Under these nutritional conditions Wt mice developed severe steatosis (Fig. 2*A*), including massive accumulation of large lipid droplets and a significant increase in liver triglyceride (TG) (Fig. 2*B*). The hCOX-2–Tg mice were protected against liver steatosis, showing fewer and smaller lipid droplets, whereas DFU administration partially reverted this effect, exhibiting an intermediate liver steatosis but including lipids microvesicles (Supplementary Fig. 3*A*). The steatosis score, as defined by Nonalcoholic Steatohepatitis Clinical Research Network Scoring System Definitions (17), was lower in hCOX-2–Tg mice (Supplementary Fig. 3*B*).

COX-2–Tg Mice Are Protected From Hepatic Inflammation and Injury

Because the increase in adipose tissue and inflammation has been linked to IR, we performed histologic examination of eWAT, and the results showed adipocyte hypertrophy with larger adipocytes in Wt mice versus hCOX-2–Tg; and again, COX-2–Tg mice treated with DFU resembled features of the Wt eWAT (Fig. 2*C*). A frequency histogram showed a shift to the left in adipocyte size in the hCOX-2–Tg mice, with a significant increase in the number of cells and a decrease in the occupied area (mean 1,168 ± 652 μm^2 for Wt and 624 ± 356 μm^2 for hCOX-2–Tg, $P < 0.05$); this process was partially reverted with the DFU treatment (748 ± 863 μm^2) (Fig. 2*D* and *E*). Moreover, as an estimation of body fat content, eWAT plus iWAT mass referred to body weight was lower in hCOX-2–Tg mice, whereas tibia length did not change between Wt and hCOX-2–Tg mice (Fig. 2*F*). These results indicate hypertrophy in eWAT from Wt mice. Cytokine eWAT expression is shown in Fig. 2*G*. As expected, higher adiponectin levels were detected in hCOX-2–Tg mice together with a significant decrease in the proinflammatory markers tumor necrosis factor-α (TNF-α) and interleukin (IL)-6.

Indeed, whereas plasma TGs were significantly elevated exclusively in obese Wt mice after the HFD, plasma cholesterol increased both in Wt and hCOX-2–Tg mice. Levels of plasma nonesterified fatty acids (NEFA) were higher in HFD-fed Wt mice than in hCOX-2–Tg mice (Table 1). Plasma insulin and leptin increased after the HFD in Wt mice, but smaller increases were found in hCOX-2–Tg mice. Furthermore, hCOX-2–Tg mice were hypoleptinemic under the RCD condition (Table 1), and adiponectin levels were elevated (20% increase) in hCOX-2–Tg mice versus Wt controls under the HFD condition. The adiponectin-to-leptin ratio was higher in hCOX-2–Tg; however, HOMA-IR was lower in hCOX-2–Tg mice under the HFD condition (Table 1). DFU treatment in the hCOX-2–Tg mice partially prevented the beneficial effects on plasmatic parameters induced by COX-2–dependent prostaglandins. In fact, plasmatic PGE_2 did not change with the HFD; however, as expected, PGE_2 levels decreased under DFU treatment (Table 1). Hepatic injury was analyzed by measuring alanine aminotransferase and aspartate aminotransferase activities, and both enzymes increased by the effect of HFD to a lesser extent in hCOX-2–Tg mice (Supplementary Fig. 4). The HFD led to a chronic inflammatory profile, which is believed to be critical for the development of glucose intolerance and IR (18). Accordingly, hepatic mRNA levels of TNF-α, Il-1β, and IL-6 were significantly enhanced in livers from HFD-fed Wt mice, whereas hCOX-2–Tg mice exhibited lower levels of these inflammatory markers (Table 2).

After detecting the differences in NEFAs levels, high-resolution magic-angle spinning magnetic resonance spectroscopy was performed to identify and quantify saturated fatty acids (Supplementary Fig. 5*A* and *B*). We found a lower value of the pool of total saturated fatty acids in hCOX-2–Tg mice compared with Wt, and this result was reversed in hCOX2–Tg+DFU (Supplementary Fig. 5*B*).

To gain insight into the molecular mechanisms implicated in COX-2 protection, we evaluated mRNA levels of transcription factors and genes involved in fatty acid oxidation, lipolysis, and lipogenesis. In hCOX-2–Tg liver, there was a significant increase of *Ppara* and *Cpt1a* under the HFD condition indicating an enhanced fatty acid oxidation. In agreement, the expression levels of genes involved in fatty acid synthesis, such as *Pparg* and *Scd1*, were markedly increased in Wt, but upregulation of these markers was lower in hCOX-2–Tg mice. Also, *Cd36* expression was lower in hCOX-2–Tg. Moreover, gene expression of COX-2–mediated responsive primary targets has been analyzed. As expected, hCOX-2–Tg mice showed an increase

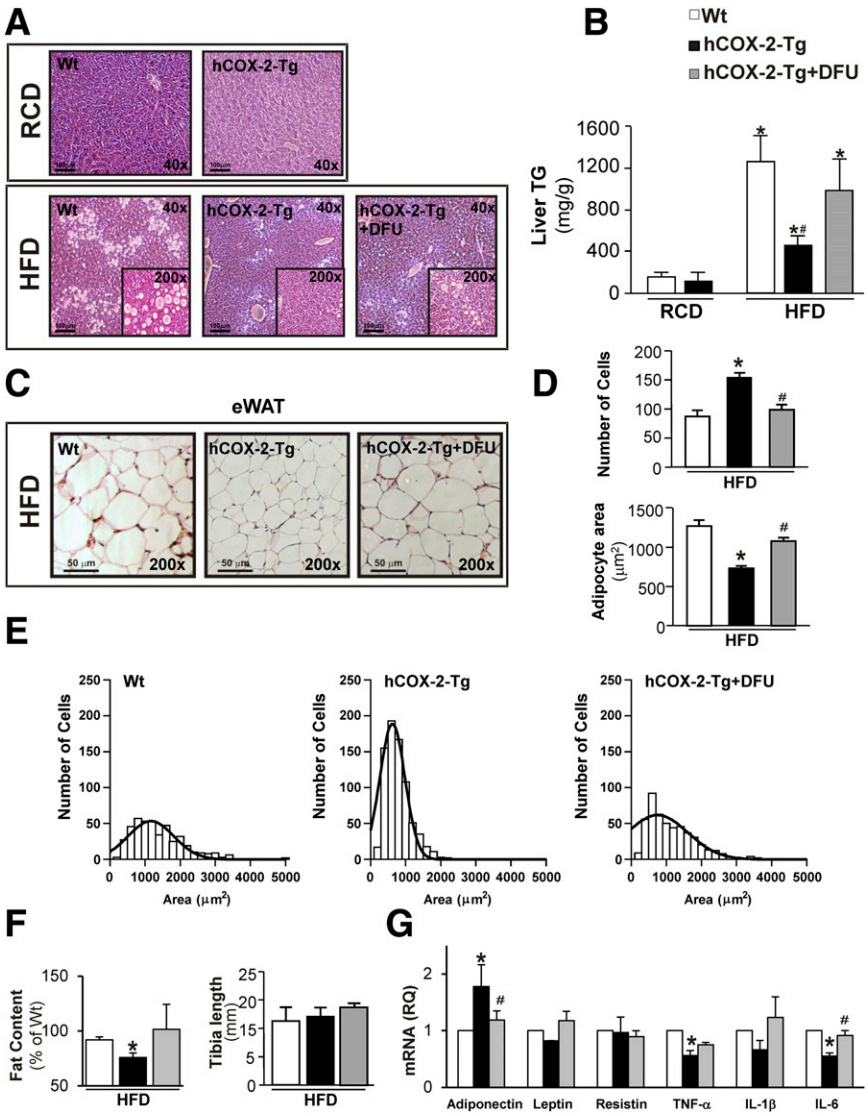

Figure 2—COX-2–Tg mice are protected from HFD-induced hepatic steatosis. *A*: Representative images of hematoxylin and eosin (H&E)-stained liver paraffin-embedded sections from Wt and hCOX-2–Tg mice under RCD and from Wt, hCOX-2–Tg, and hCOX-2–Tg+DFU mice under the HFD condition. *B*: Hepatic TG levels in all experimental groups, measured by enzymatic analysis. Data are expressed as means ± SE ($n = 7$ per group). *$P < 0.05$ vs. Wt-RCD; #$P < 0.05$ vs. Wt-HFD. *C*: Representative images of H&E-stained sections of paraffin-embedded eWAT from Wt, hCOX-2–Tg, and hCOX-2–Tg+DFU mice under the HFD condition. *D*: Number and adipocyte area expressed in μm^2 of five sections per animal ($n = 4$ per group). *E*: Frequency histograms of eWAT from HFD-fed Wt, hCOX-2–Tg, and hCOX-2–Tg+DFU mice. *F*: eWAT + iWAT fat mass content related to body weight and tibia length. *G*: mRNA levels of adipokines and proinflammatory cytokines measured in eWAT by real-time quantitative PCR and normalized to the expression of 36b4 mRNA. Values represent fold relative to Wt under the HFD condition. Data are expressed as means ± SE for four to six mice for each experimental group. *$P < 0.05$ vs. Wt-HDF; #$P < 0.05$ vs. hCOX-2–Tg-HFD.

in hepatic mRNA levels of *CyclinD1* and *Bcl2*, known target genes of COX-2, and *mPges1*, the second key enzyme that couples with COX-2 for the synthesis of PGE_2 (Table 3).

Increased EE in COX-2–Tg Mice After HFD Treatment

To determine the cause of decreased adiposity and improved insulin sensitivity in hCOX-2–Tg mice, we examined food intake and EE. The reduced adiposity of hCOX-2–Tg mice could not be explained by decreased food intake (Fig. 1*D*) but was associated with increased EE. Of note, no differences were found in basal rectal temperature by a possible pyrogenic effect of PGE_2 (Wt: 36.4 ± 0.6°C; h-COX-2–Tg: 35.8 ± 0.7°C).

VO_2 was elevated in hCOX-2–Tg mice versus Wt mice during light and dark cycles. As expected, DFU treatment of hCOX-2–Tg resembled the Wt situation (Fig. 3*A* and Supplementary Fig. 6*A*). Similar results were obtained when CO_2 production was measured, and as a consequence, EE and RER were also increased in hCOX-2–Tg mice versus Wt mice during light and dark periods (Fig. 3*B*, *C* and *E* and Supplementary Fig. 6*E*). However, no differences between genotypes were noted in locomotor activity (Fig. 3*D*).

Table 1—Biochemical and metabolic characteristics of hCOX-2–Tg mice after HFD

	RCD		HFD		
	Wt	hCOX-2–Tg	Wt	hCOX-2–Tg	hCOX-2–Tg+DFU
TG (mg/dL)	23.80 ± 2.70	23.66 ± 4.51	35.78 ± 3.08*	23.28 ± 1.89#	32.59 ± 1.63*†
Cholesterol (mg/dL)	101.78 ± 12.98	72.71 ± 10.72	232.17 ± 25.68*	147.78 ± 9.13z*#	207.90 ± 15.33*†
NEFAs (mEq/L)	18.69 ± 2.21	16.79 ± 2.77	23.44 ± 2.96*	14.17 ± 2.43#	21.69 ± 4.42*†
Insulin (ng/mL)	0.94 ± 0.30	0.72 ± 0.17	1.73 ± 0.36*	1.46 ± 0.13*	2.23 ± 0.66*
Adiponectin (pg/mL)	7.21 ± 0.72	6.99 ± 1.64	6.08 ± 1.11	8.05 ± 0.35#	4.94 ± 0.61*†
Leptin (pg/mL)	7.61 ± 2.07	3.82 ± 0.64*	24.93 ± 1.81*	21.29 ± 1.49*#	24.95 ± 0.89*†
Adiponectin-to-leptin ratio	0.95	1.83*	0.24	0.38#	0.20
HOMA-IR (AU)			19.01 ± 2.89	14.46 ± 0.92#	23.43 ± 0.63
PGE_2 (pg/mL)	9.43 ± 1.16	14.18 ± 1.10*	8.98 ± 0.35	12.04 ± 0.48*#	8.03 ± 0.34†

Plasma levels of TGs, cholesterol, NEFAs, insulin, leptin, and adiponectin from Wt, hCOX-2–Tg, and hCOX-2–Tg+DFU mice fed the RCD or the HFD for 12 weeks. The adiponectin-to-leptin ratio, HOMA-IR, plasma PGE_2 levels from Wt, hCOX-2–Tg, and hCOX-2–Tg+DFU mice fed with the RCD or HFD. Data are expressed as means ± SE for four to six mice of each experimental group. *$P < 0.05$ vs. Wt-RCD. #$P < 0.05$ vs. Wt-HFD. †$P < 0.05$ vs. hCOX-2–Tg–HFD. AU, arbitrary units.

In agreement with increased cage temperature (Fig. 3*F*), hepatic COX-2–derived PGE_2 enhanced the expression of thermogenic genes (*Ucp1*, *Dio2*, and *Prdm16*) in iWAT, suggesting induction of browning. Furthermore, thermogenic-gene expression was also increased in BAT in hCOX-2–Tg mice (Fig. 4*A*). To reinforce these data, we performed a cold acclimation experiment to assess the differential thermogenic response between Wt and hCOX-2–Tg mice. As shown in Fig. 4*B*, cold-induced *Ucp1*, *Dio2*, and *Prdm16* mRNA levels were significantly higher in iWAT of hCOX-2–Tg mice, suggesting a browning process. In BAT, the differential effects after cold exposure were found in *Ucp1* mRNA levels. These data reinforce the beneficial effects found in energy expenditure in hCOX-2–Tg mice. Also, PGE_2 was able to induce uncoupling protein 1 (UCP-1) expression in nondifferentiated BAT SVF cells (Fig. 4*C*).

Hepatic COX-2 Expression Enhances Insulin Signaling in Liver After HFD

The phosphorylation of Akt and AMPK-α were markedly reduced in obese Wt liver compared with hCOX-2–Tg mice (Fig. 5*A* and *B*). These differences in insulin signaling between Wt and hCOX-2–Tg mice after HFD could reflect differential expression of negative modulators of the early steps of insulin signaling. In this regard, PTP1B protein levels were upregulated in the liver of HFD-fed Wt mice compared with similar genotype fed the RCD, whereas this effect was not observed in hCOX-2–Tg mice. All of these data suggest that hCOX-2–Tg mice are protected against IR under the HFD condition.

Human and Mouse Liver Cells Expressing COX-2–Tg Are Protected Against Fatty Acids Exposure

To confirm whether liver cells expressing COX-2 exhibit higher insulin sensitivity and are protected against IR, CHL (human) and NCL (murine) cells, with (CHL-C, NCL-C) or without (CHL-V, NCL-V) COX-2 expression were treated with 600 μmol/L palmitate for 16 h and then stimulated with 10 nmol/L insulin for 15 min. As shown in Supplementary Fig 7*A–C*, CHL-C and NCL-C cells per se showed a higher increase in Akt phosphorylation in response to insulin than CHL-V and NCL-V cells. Moreover, when cells were treated with palmitate to induce IR, CHL-C and NCL-C exhibited a higher Akt phosphorylation in response to insulin than CHL-V and NCL-V, thus reinforcing the results obtained in vivo in hCOX-2–Tg mice.

DISCUSSION

The current study has demonstrated that constitutive expression of COX-2 in hepatocytes protects against steatosis, adiposity, inflammation, and hepatic IR in mice under HFD, implicating the lack of COX-2 expression under these circumstances as a novel key player in

Table 2—Hepatic mRNA expression of proinflammatory cytokines in hCOX-2–Tg mice

	RCD		HFD		
Gene	Wt	hCOX-2–Tg	Wt	hCOX-2–Tg	hCOX-2–Tg+DFU
Tnfa	1	0.65 ± 0.32	2.36 ± 0.79*	1.13 ± 0.38#	1.55 ± 0.66
Il1b	1	1.47 ± 0.30	3.16 ± 1.01*	1.52 ± 0.26#	1.47 ± 0.88
Il6	1	0.44 ± 0.10*	2.16 ± 0.68*	0.63 ± 0.20#	1.67 ± 0.81

Hepatic mRNA levels of proinflammatory cytokines IL-6, IL-1β, and TNF-α measured by real-time quantitative PCR normalized to the expression of 36b4 mRNA. Values represent fold relative to Wt under the RCD condition. Data are expressed as means ± SE for four to six mice of each experimental group. *$P < 0.05$ vs. Wt-RCD. #$P < 0.05$ vs. Wt-HFD.

Table 3—Hepatic mRNA expression of genes related to lipogenesis, lipolysis, and β-oxidation in hCOX-2–Tg mice

	RCD		HFD	
Gene	Wt	hCOX-2–Tg	Wt	hCOX-2–Tg
Cpt1a	1	1.15 ± 0.04	1.70 ± 0.20*	2.87 ± 0.27*#
Pgc1a	1	0.68 ± 0.22	1.00 ± 0.13	0.99 ± 0.14
Acox1	1	0.73 ± 0.20	1.92 ± 0.24*	1.18 ± 0.39
Ppara	1	1.61 ± 0.18*	2.54 ± 0.10*	4.41 ± 0.14*#
Pparg	1	0.16 ± 0.04*	5.95 ± 0.09*	2.94 ± 0.07*#
Acaca	1	0.94 ± 0.18	1.21 ± 0.36	0.89 ± 0.16
Fasn	1	1.59 ± 0.43	1.32 ± 0.72	1.09 ± 0.35
Scd1	1	0.64 ± 0.24	2.25 ± 0.23*	1.46 ± 0.09*#
Lipc	1	0.87 ± 0.17	1.05 ± 0.18	1.18 ± 0.16
Lipe	1	0.82 ± 0.08	1.70 ± 0.06*	1.80 ± 0.56
Pnpla2	1	0.97 ± 0.17	1.68 ± 0.56	2.55 ± 0.53
Cd36	1	0.67 ± 0.18	6.30 ± 0.38*	3.65 ± 0.22*#
hcox2	1	7,365.5 ± 453.8*	1.04 ± 0.43	6,749.9 ± 266.2*#
mpges1	1	1.58 ± 0.39	0.84 ± 0.35	1.68 ± 0.32*#
CyclinD1	1	1.34 ± 0.08*	1.10 ± 0.21	1.51 ± 0.25*#
Bcl2	1	1.13 ± 0.11	0.96 ± 0.20	1.57 ± 0.35*#

Hepatic mRNA levels measured by real-time quantitative PCR normalized to the expression of 36b4 mRNA. Values represent fold relative to Wt under the RCD condition. Data are expressed as means ± SE for four to six mice of each experimental group. *$P < 0.05$ vs. Wt-RCD. #$P < 0.05$ vs. Wt-HFD.

the development of obesity-associated metabolic dysfunction. Importantly, the leanness of hCOX-2–Tg mice is associated with increased systemic EE, enhanced thermogenesis, and fatty acid oxidation in the liver. Furthermore, pharmacological inhibition of COX-2 with DFU reverts to the situation of the Wt mice.

Our previous results (12), by using this transgenic model, demonstrated a protective role of COX-2 against liver injury in an experimental model of streptozotocin-mediated hyperglycemia. The current study reveals that hCOX-2–Tg mice exhibit increased insulin sensitivity in basal conditions and after HFD and are protected against HFD-induced glucose intolerance, steatosis, and adiposity. Recent studies suggested that COX-2 expression in eWAT protects against obesity by an increase in thermogenic activity (19). Moreover, this effect has been attributed principally to COX-2–derived PGE_2 (20). In agreement with this, the reduced adiposity found in hCOX-2–Tg mice under HFD could be explained as a consequence of elevated EE caused by increased substrate consumption. In this way, circulating liver-derived PGE_2 might be sufficient for the induction of thermogenic genes in adipose tissues, all of these contributing to protection against HFD-induced obesity and improvement of glucose homeostasis. This was supported by the enhanced thermogenic gene expression found in iWAT and BAT of hCOX-2–Tg mice under the HFD condition or cold exposure and by the induction of UCP-1 protein levels in brown preadipocytes stimulated with PGE_2.

Elevation of circulating fatty acids and proinflammatory adipokines secreted by WAT reduces insulin sensitivity in liver and skeletal muscle (21), and adipose tissue inflammation has been correlated with hepatic steatosis in humans (22). Our results show that hCOX-2–Tg mice did not develop the common increase in fat mass and enhanced adipocyte hypertrophy that is shown in Wt mice under the HFD condition. In agreement with these data, plasma and hepatic TGs, cholesterol, and NEFAs levels were lower in hCOX-2–Tg mice, and these mice also showed decreased plasma insulin and leptin and increased adiponectin levels. Moreover, proinflammatory markers were also lower in hepatic tissue from hCOX-2–Tg mice compared with Wt after the HFD. Altogether, these parameters indicate that the beneficial effects on obesity and glucose homeostasis in hCOX-2–Tg mice might be due to decreased inflammation.

When Wt and hCOX-2–Tg mice were fed the HFD, we found an important protection against steatosis and IR versus Wt mice. Moreover, we found significant differences in the expression of key enzymes and transcription factors implicated in lipogenesis and β-oxidation, such as *Pparg*, *Scd1*, *Ppara*, *Cpt1a*, and *CD36*, indicating an increase in β-oxidation in hCOX-2–Tg mice under the HFD condition. Recent results have implicated hepatic fatty acid translocase CD36 upregulation with IR and steatosis in nonalcoholic steatohepatitis and chronic hepatitis C (23). In addition, the positive effects of COX-2 on inflammation and IR are evidenced by the prevention of obesity through increased EE and RER.

The phosphatidylinositide 3-kinase/Akt and AMPK pathways play a central role in integrating diverse survival

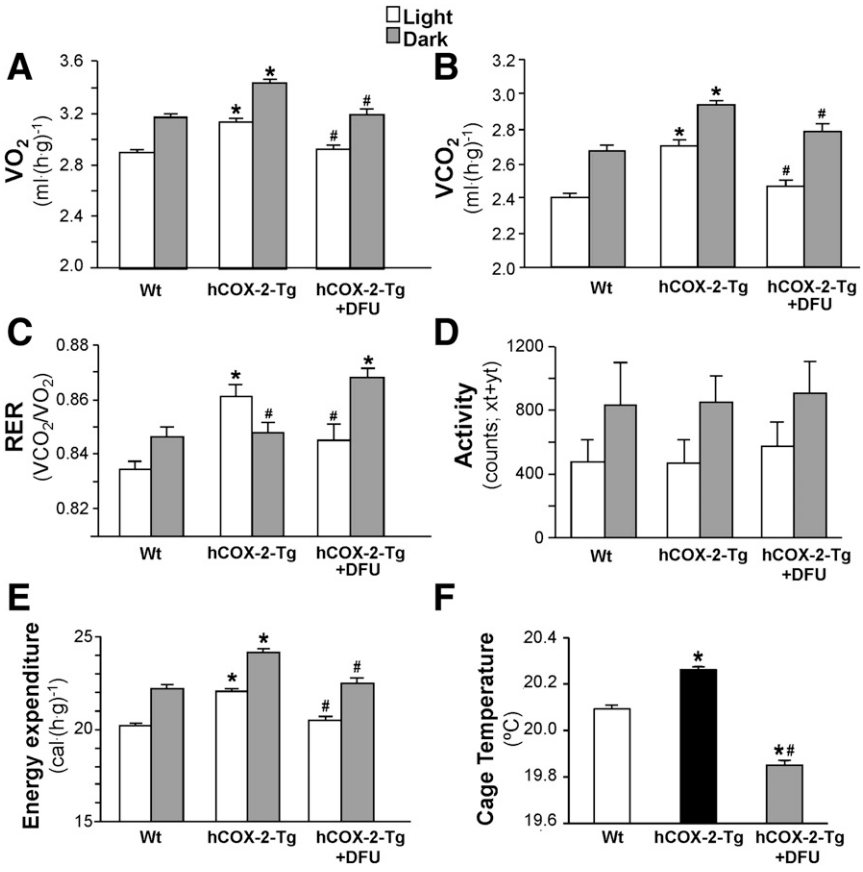

Figure 3—Increased energy expenditure in hCOX-2–Tg mice under the HFD condition. VO_2 (*A*), VCO_2 (*B*), RER (*C*), locomotor activity (*D*), EE (*E*), and average cage temperature (*F*) in HFD-fed Wt, hCOX-2–Tg, and hCOX-2–Tg+DFU mice were measured in 12-h light/dark cycles. Data are expressed as means ± SE for four mice in each experimental group. **P* < 0.05 vs. Wt-HDF; #*P* < 0.05 vs. hCOX-2–Tg-HFD.

signals. Moreover, Akt phosphorylation is a critical node of the insulin-signaling pathway, being that tyrosine-phosphorylated insulin receptor substrate-1 is an upstream mediator of its activation (1). It is known that the Akt pathway is a target of prostaglandins and that Akt phosphorylation is enhanced in the liver of hCOX-2–Tg mice compared with the Wt mice, thus reinforcing the survival pathways (12). In Wt liver, the HFD impaired insulin-stimulated Akt phosphorylation, and this effect was prevented in hCOX-2–Tg mice. This situation was paralleled in murine- and human-derived liver cells overexpressing COX-2. The increase in the phosphorylated (p)Akt-to-Akt ratio in hCOX-2–Tg mice under RCD and HFD conditions may be due, besides intracellular signaling, to a direct Akt activation through COX-2–dependent PGE_2 acting via EP2/EP4 Gβγ dimers, as reported by Rizzo (24). Notably, the effect of PGE_2 pretreatment on Akt phosphorylation observed in isolated hepatocytes confirmed that COX-2–derived prostanoids can be responsible for this effect. Thus, the improved insulin sensitivity in vivo reflected by hepatic Akt activation found in hCOX-2–Tg mice might contribute to the amelioration of HFD-derived deleterious metabolic effects as exacerbated lipogenesis and hepatic TG content.

AMPK-α1 is known to protect mice from diet-induced obesity and IR. AMPK-α1 knockdown in mice enhanced adipocyte lipid accumulation, exacerbated the inflammatory response, and induced IR (25). We showed that AMPK was phosphorylated in liver cells expressing COX-2 under basal conditions and after liver injury (16). Indeed, AMPK phosphorylation and its downstream gene *Cpt1a,* which regulates a rate-controlling step of fatty acid oxidation transferring long-chain acyl-CoA into the mitochondria, were increased in hCOX-2–Tg mice under the HFD condition. Cellular lipid content is determined by the balance between fatty acid oxidation and lipid storage as TGs. Because the ability of AMPK to induce lipid oxidation is considered an important feature for insulin sensitization (26), this might also contribute to the beneficial effects of COX-2 expression in hepatocytes on insulin sensitivity.

In addition to the molecular mechanisms mentioned above, differences in insulin signaling between Wt and hCOX-2–Tg mice after the HFD could reflect differential expression of negative modulators of the early steps of insulin signaling. Among them, PTP1B was a likely candidate given its ability to directly dephosphorylate the insulin receptor and its expression being induced by

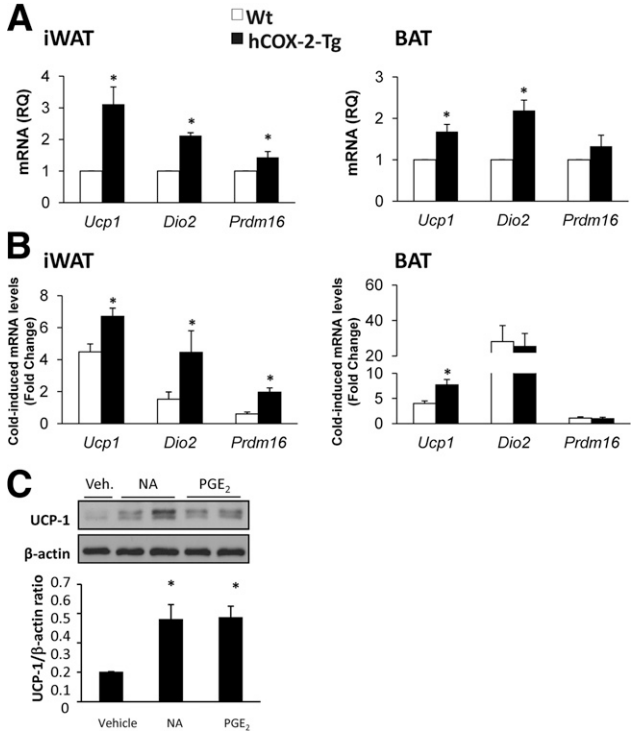

Figure 4—Enhanced thermogenic-related genes in hCOX-2–Tg mice. *A*: *Ucp1, Dio2,* and *Prdm16* mRNA levels were measured in iWAT and BAT by real-time quantitative PCR and normalized to the expression of 36b4 mRNA. Values represent fold relative to Wt under the HFD condition. Data are expressed as means ± SE for six mice of each experimental group. **P* < 0.05 vs. Wt-HFD. *B*: Mice were maintained at 28°C for 1 week and then at 4°C for 6 h. *Ucp1*, *Dio2*, and *Prdm16* mRNA levels were measured in iWAT and BAT by real-time quantitative PCR and normalized to the expression of 36b4 mRNA. Results are means ± SE for four to six mice of each experimental group. Data are expressed as fold change relative to Wt or hCOX-2–Tg at thermoneutrality. **P* < 0.05 vs. cold exposure Wt. *C*: BAT precursor stromal vascular fraction cells were stimulated with PGE_2 (1 μmol/L) or noradrenalin (NA) (1 μmol/L) as a positive control for 24 h, and UCP-1 expression was analyzed by Western blot. Data are expressed as means ± SE for three different experiments. **P* < 0.05 vs. control without stimulation.

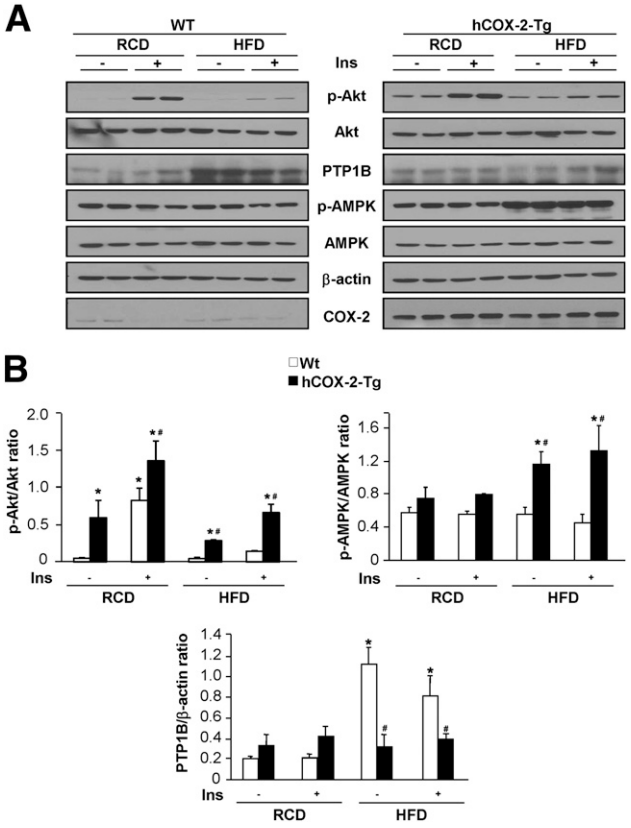

Figure 5—COX-2 expression enhances insulin signaling in liver of mice fed the HFD. *A:* Representative Western blot analysis of Wt and COX-2–Tg liver under RCD or HFD; nontreated (−Ins) or treated (+Ins) with 0.75 units/kg insulin (Ins) for 15 min before being killed. *B*: Ratios phosphorylated (p)-Akt/Akt and p-AMPK/AMPK after densitometric analysis of Western blot data normalized using β-actin as control. Data are expressed as means ± SE for four to six mice of each experimental group. **P* < 0.05 vs. Wt (−Ins); #*P* < 0.05 vs. Wt-HFD (−Ins).

inflammatory mediators (27). PTP1B-knockout mice are protected against obesity-induced inflammation and peripheral IR during aging (28). In agreement with these data, PTP1B protein was upregulated in the liver of HFD-fed Wt mice but not in hCOX-2–Tg mice, suggesting that COX-2–dependent prostaglandins might protect from the elevation of PTP1B during obesity. In addition, PTP1B modulates leptin sensitivity (29), and decreased leptin levels are found in hCOX-2–Tg mice in both RCD and HFD conditions, suggesting a possible cross talk between COX-2–derived signals and leptin.

Henkel et al. (30) reported that PGE_2 produced in Kupffer cells interrupts the intracellular insulin signaling in hepatocytes through serine phosphorylation of insulin receptor substrate-1 via EP3 receptor-dependent ERK1/2 activation. Moreover, they demonstrated that the EP3 receptor in hepatocytes is expressed at higher levels than the other isoforms (30). However, our results show that the liver of Wt and hCOX-2–Tg mice expresses comparable levels of all of the EPs receptors (EP1–4; data not shown) indicating a different molecular mechanism of action. Our in vivo data in the hCOX-2–Tg model, characterized by a continuous production of PGE_2 in the liver, clearly show enhanced insulin-mediated Akt phosphorylation partly due to decreased PTP1B levels under the HFD condition. Therefore, the view emerging from this study is that prostaglandins synthesized by other liver cells (Kupffer or stellate) are not sufficient to cope for the beneficial effects observed when hepatocytes are able to express COX-2.

In conclusion, the current study demonstrates that expression of COX-2 in hepatocytes protects against adiposity, inflammation, and hepatic IR in mice under the HFD condition, pointing to COX-2 as a potential therapeutic target against obesity-associated metabolic dysfunction. Stable analogs of PGE_2, such as 16,16dmPGE_2, resembling COX-2 overexpression (31), could be administered to treat steatosis or IR. In fact, PGE_1 and PGE_2 and

their analogs are used in the clinic to improve moderate hypercholesterolemia among other liver pathologies (32). Furthermore, these results support caution with use of COX inhibitors in patients with obesity, type 2 diabetes, or nonalcoholic fatty liver disease.

Acknowledgments. The authors thank Gerardo Pisani (Instituto de Fisiología Experimental-Consejo Nacional de Investigaciones Científicas y Técnicas), Rosario, Argentina, for his technical assistance with the immunohistochemical analysis.

Funding. This work was supported by Financing Program for Short Stays Abroad (Consejo Nacional de Investigaciones Científicas y Técnicas-Argentina) to D.E.F., by a Post-Doctoral fellowship from Consejo Nacional de Ciencia y Tecnología, México, SAF2012-39732 (Ministerio de Economía y Competitividad [MINECO], Spain) to L.C.-S., by CIBERehd (Instituto de Salud Carlos III [ISCIII], Spain) to M.C., by BFU2011-24760 (MINECO, Spain) to L.B., by S2010/BMD-2378 (Comunidad de Madrid) to L.B. and P.M.-S., by RD12/0042/0019 (ISCIII, Spain) and CIBERehd (ISCIII, Spain) to L.B. and P.M.-S., by SAF2010-16037, SAF2013-43713-R (MINECO, Spain) to P.M.-S., and by SAF2012-33283 (MINECO, Spain), S2010/BMD-2423 (Comunidad de Madrid), European Foundation for the Study of Diabetes and Amylin Paul Langerhans Grant, and CIBERDEM (ISCIII, Spain) to Á.M.V.

Duality of Interest. No potential conflicts of interest relevant to this article were reported.

Author Contributions. D.E.F., O.M., N.A., Á.G.-R., A.F-Á., C.C., E.G.-C., and Á.M.V. researched the data. L.C.-S. edited the manuscript. R.M., L.B., C.E.C., and M.C. reviewed the manuscript and contributed to discussion. Á.M.V. and P.M-S. wrote and reviewed the manuscript. Á.M.V. and P.M.-S. are the guarantors of this work and, as such, had full access to all the data in the study and take responsibility for the integrity of the data and the accuracy of the data analysis.

References

1. Tilg H, Moschen AR. Inflammatory mechanisms in the regulation of insulin resistance. Mol Med 2008;14:222–231
2. Rosen ED, Spiegelman BM. Adipocytes as regulators of energy balance and glucose homeostasis. Nature 2006;444:847–853
3. Copps KD, White MF. Regulation of insulin sensitivity by serine/threonine phosphorylation of insulin receptor substrate proteins IRS1 and IRS2. Diabetologia 2012;55:2565–2582
4. Simmons DL, Botting RM, Hla T. Cyclooxygenase isozymes: the biology of prostaglandin synthesis and inhibition. Pharmacol Rev 2004;56:387–437
5. Callejas NA, Boscá L, Williams CS, DuBois RN, Martín-Sanz P. Regulation of cyclooxygenase 2 expression in hepatocytes by CCAAT/enhancer-binding proteins. Gastroenterology 2000;119:493–501
6. Casado M, Callejas NA, Rodrigo J, et al. Contribution of cyclooxygenase 2 to liver regeneration after partial hepatectomy. FASEB J 2001;15:2016–2018
7. Martín-Sanz P, Callejas NA, Casado M, Díaz-Guerra MJ, Boscá L. Expression of cyclooxygenase-2 in foetal rat hepatocytes stimulated with lipopolysaccharide and pro-inflammatory cytokines. Br J Pharmacol 1998;125:1313–1319
8. Hsieh PS, Jin JS, Chiang CF, Chan PC, Chen CH, Shih KC. COX-2-mediated inflammation in fat is crucial for obesity-linked insulin resistance and fatty liver. Obesity (Silver Spring) 2009;17:1150–1157
9. Hsieh PS, Tsai HC, Kuo CH, et al. Selective COX2 inhibition improves whole body and muscular insulin resistance in fructose-fed rats. Eur J Clin Invest 2008;38:812–819
10. Tian YF, Hsia TL, Hsieh CH, Huang DW, Chen CH, Hsieh PS. The importance of cyclooxygenase 2-mediated oxidative stress in obesity-induced muscular insulin resistance in high-fat-fed rats. Life Sci 2011;89:107–114
11. Coll T, Palomer X, Blanco-Vaca F, et al. Cyclooxygenase 2 inhibition exacerbates palmitate-induced inflammation and insulin resistance in skeletal muscle cells. Endocrinology 2010;151:537–548
12. Francés DE, Ingaramo PI, Mayoral R, et al. Cyclooxygenase-2 overexpression inhibits liver apoptosis induced by hyperglycemia. J Cell Biochem 2013;114:669–680
13. Casado M, Mollá B, Roy R, et al. Protection against Fas-induced liver apoptosis in transgenic mice expressing cyclooxygenase 2 in hepatocytes. Hepatology 2007;45:631–638
14. Llorente Izquierdo C, Mayoral R, Flores JM, et al. Transgenic mice expressing cyclooxygenase-2 in hepatocytes reveal a minor contribution of this enzyme to chemical hepatocarcinogenesis. Am J Pathol 2011;178:1361–1373
15. Trusca VG, Fuior EV, Florea IC, Kardassis D, Simionescu M, Gafencu AV. Macrophage-specific up-regulation of apolipoprotein E gene expression by STAT1 is achieved via long range genomic interactions. J Biol Chem 2011;286:13891–13904
16. Mayoral R, Mollá B, Flores JM, Boscá L, Casado M, Martín-Sanz P. Constitutive expression of cyclo-oxygenase 2 transgene in hepatocytes protects against liver injury. Biochem J 2008;416:337–346
17. Kleiner DE, Brunt EM, Van Natta M, et al.; Nonalcoholic Steatohepatitis Clinical Research Network. Design and validation of a histological scoring system for nonalcoholic fatty liver disease. Hepatology 2005;41:1313–1321
18. Hotamisligil GS. Inflammation and metabolic disorders. Nature 2006;444:860–867
19. Vegiopoulos A, Müller-Decker K, Strzoda D, et al. Cyclooxygenase-2 controls energy homeostasis in mice by de novo recruitment of brown adipocytes. Science 2010;328:1158–1161
20. García-Alonso V, López-Vicario C, Titos E, et al. Coordinate functional regulation between microsomal prostaglandin E synthase-1 (mPGES-1) and peroxisome proliferator-activated receptor γ (PPARγ) in the conversion of white-to-brown adipocytes. J Biol Chem 2013;288:28230–28242
21. Olefsky JM. Fat talks, liver and muscle listen. Cell 2008;134:914–916
22. Cancello R, Tordjman J, Poitou C, et al. Increased infiltration of macrophages in omental adipose tissue is associated with marked hepatic lesions in morbid human obesity. Diabetes 2006;55:1554–1561
23. Miquilena-Colina ME, Lima-Cabello E, Sánchez-Campos S, et al. Hepatic fatty acid translocase CD36 upregulation is associated with insulin resistance, hyperinsulinaemia and increased steatosis in non-alcoholic steatohepatitis and chronic hepatitis C. Gut 2011;60:1394–1402
24. Rizzo MT. Cyclooxygenase-2 in oncogenesis. Clin Chim Acta 2011;412:671–687
25. Zhang W, Zhang X, Wang H, et al. AMP-activated protein kinase α1 protects against diet-induced insulin resistance and obesity. Diabetes 2012;61:3114–3125
26. Yamauchi T, Kamon J, Minokoshi Y, et al. Adiponectin stimulates glucose utilization and fatty-acid oxidation by activating AMP-activated protein kinase. Nat Med 2002;8:1288–1295
27. Zabolotny JM, Kim YB, Welsh LA, Kershaw EE, Neel BG, Kahn BB. Protein-tyrosine phosphatase 1B expression is induced by inflammation in vivo. J Biol Chem 2008;283:14230–14241
28. González-Rodríguez A, Más-Gutierrez JA, Mirasierra M, et al. Essential role of protein tyrosine phosphatase 1B in obesity-induced inflammation and peripheral insulin resistance during aging. Aging Cell 2012;11:284–296
29. Zabolotny JM, Bence-Hanulec KK, Stricker-Krongrad A, et al. PTP1B regulates leptin signal transduction in vivo. Dev Cell 2002;2:489–495
30. Henkel J, Neuschäfer-Rube F, Pathe-Neuschäfer-Rube A, Püschel GP. Aggravation by prostaglandin E2 of interleukin-6-dependent insulin resistance in hepatocytes. Hepatology 2009;50:781–790
31. Madsen L, Pedersen LM, Lillefosse HH, et al. UCP1 induction during recruitment of brown adipocytes in white adipose tissue is dependent on cyclooxygenase activity. PLoS ONE 2010;5:e11391
32. Korhonen T, Savolainen MJ, Jääskeläinen T, Kesäniemi YA. Effect of a synthetic prostaglandin E2 analogue, RS-86505-007, on plasma lipids and lipoproteins in patients with moderate hypercholesterolaemia: efficacy and tolerance of treatment and response in different apolipoprotein polymorphism groups. Eur J Clin Pharmacol 1995;48:97–102